

Precision Measurement of the e^- and e^+ Fluxes in Primary Cosmic Rays with the Alpha Magnetic Spectrometer on the International Space Station

Valerio Vagelli^{*†}

University of Perugia – Istituto Nazionale di Fisica Nucleare, Sezione di Perugia

E-mail: valerio.vagelli@pg.infn.it

The measurements of the cosmic ray e^\pm and $(e^+ + e^-)$ fluxes based on the analysis of the first 30 months of data collected by the AMS-02 detector onboard the International Space Station is reviewed. The collected statistics and the resolution of the detector provide unprecedented accuracy in the analysis of the energy dependence of the e^\pm and the $(e^+ + e^-)$ fluxes and of the positron fraction. The results provide new interesting information on the properties of e^\pm cosmic rays.

38th International Conference on High Energy Physics

3-10 August 2016

Chicago, USA

^{*}Speaker.

[†]for the AMS collaboration.

The Alpha Magnetic Spectrometer (AMS-02) is the high energy spectrometer experiment operating on the International Space Station since May 2011 to conduct a long duration mission of direct measurements in space of cosmic ray (CR) spectra and composition up to the TeV energy scale. Direct measurements of the e^\pm fluxes up to the TeV energies provide important information on the origin and propagation of CRs. Being the lightest charged CR component, the e^\pm spectra are sensitive to the features of the local propagation medium. Moreover, the accurate analysis of the relative e^+ and e^- abundances and of their energy spectral shapes could reveal signatures of CR e^\pm exotic sources, like e^\pm production from Dark Matter (DM) annihilation in the Galaxy or from nearby astrophysical sources (pulsars and SuperNovæ Remnants). In the following, the most recent AMS-02 measurements of e^\pm in CRs are reviewed. Additional details are available in [1].

1. The AMS-02 detector

The AMS-02 detector is fully described in [2]. Its core consists of the magnetic spectrometer, composed of a permanent magnet generating a 0.14 T dipolar magnetic field and 9 layers of double sided silicon microstrip tracker detectors with $10\ \mu\text{m}$ position resolution in the magnetic field bending direction. The measurement of the energy deposits in the tracker layers is used to determine the particle absolute charge, Z . The layer crossing coordinates determine the particle trajectory and curvature in the magnetic field. The particle rigidity $R = p/Z$, where p is the momentum, is measured over a lever arm up to 3 m. The maximum detectable rigidity for $|Z| = 1$ particles is 2 TV. Four time of flight (TOF) planes trigger the readout of the detector and measure the particle flight direction and velocity with a time of flight resolution of 160 ps. An anti-coincidence veto system located inside the magnet bore rejects particles outside the acceptance of the detector with inefficiency lower than 10^{-5} . To improve the particle identification capabilities, AMS-02 is equipped from top to bottom with a transition radiation detector (TRD), a ring imaging Cherenkov detector (RICH) and an electromagnetic calorimeter (ECAL). The $17X_0$ ECAL provides the accurate measurement of the e^\pm energy scaled to the top of the detector (E). Its 3-dimensional imaging capabilities for the reconstruction of the shower development is exploited to separate e^\pm from hadrons. The energy deposit in the 20 layers of proportional tubes in the TRD are exploited to further differentiate between e^\pm and protons. The magnet, located between TRD and ECAL, ensures that the information provided by the two subdetectors are independent from each other.

2. Data Analysis

AMS-02 collected $\sim 41 \times 10^9$ events from 19 May 2011 to 26 Nov. 2013. The data have been analyzed to measure the positron fraction (PF, $e^+/(e^+ + e^-)$) and the e^- , e^+ and $(e^+ + e^-)$ fluxes. The fluxes are measured for each energy bin of width ΔE as:

$$\Phi(E) = \frac{N(E)}{A(E) \cdot \epsilon_{\text{trig}}(E) \cdot \Delta T(E) \cdot \Delta E} \quad (2.1)$$

where A is the effective detector acceptance, ϵ_{trig} is the trigger efficiency and ΔT is the exposure time; N are the events identified as e^\pm , after rejection of secondary particles of atmospheric origin.

The PF measurement is affected by lower systematic uncertainties than the flux measurements, because most of the normalization factors cancel out in the fraction. The advantage of the $(e^+ + e^-)$ flux measurement – which does not require any selection on the sign of the curvature – is the higher selection efficiency. Its measurement results in improved statistical and systematic uncertainties and in an extended energy range than what obtained for the separate e^\pm flux measurements.

The identification of the e^\pm signal and the separation from the overwhelming proton background is achieved combining the hadronic rejection capabilities of the independent ECAL and TRD subdetectors (Fig. 1). An ECAL classifier, based on a Boosted Decision Tree algorithm, is used to differentiate e^\pm from protons by exploiting their different shower shapes. To further separate e^\pm and protons, the signals in the TRD layers are combined into a TRD classifier based on the likelihood probabilities of the e^\pm and proton hypotheses. The comparison of the ECAL energy and the spectrometer rigidity measurements (E/R) improves the proton rejection capabilities.

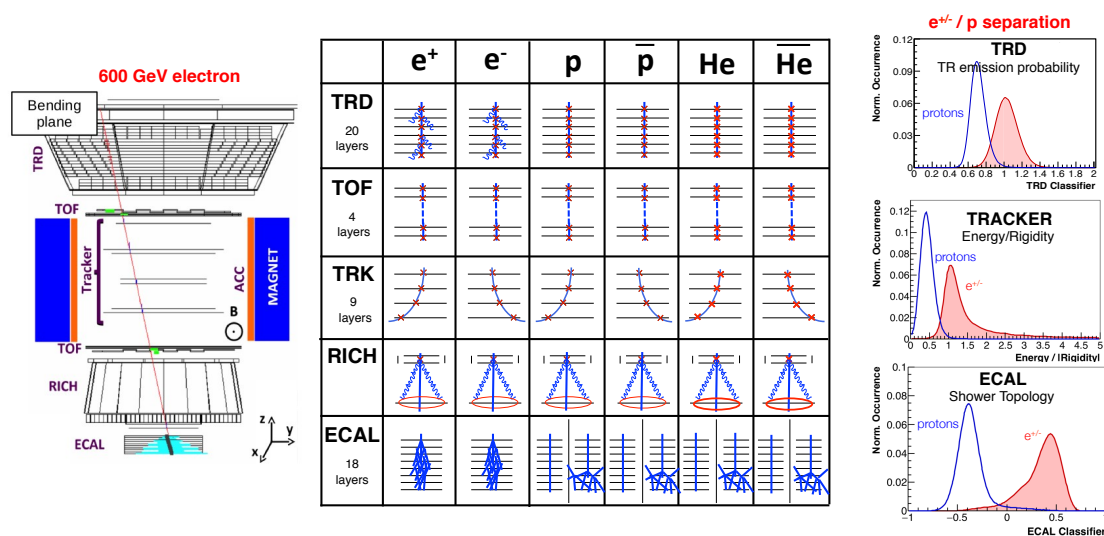


Figure 1: Left: Event display for a 600 GeV electron detected by AMS-02. Center: Particle identification capabilities for each subdetector. Right: TRD, Tracker and ECAL classifier distributions for e^\pm and protons.

Data-driven methods have been exploited to evaluate the amount of e^\pm in the data. The procedure for the evaluation of the $(e^+ + e^-)$ component will be described, and similar approaches have been applied in the different e^\pm analyses. A selection based on the TRD, tracker and TOF subdetectors has been applied to identify downward-going relativistic $|Z|=1$ particles in the TRD and ECAL acceptance. Secondary particles of atmospheric origin are rejected with requirements on the geomagnetic rigidity cutoff. The majority of protons, that dominate the selected $|Z|=1$ sample, is removed with a selection on the ECAL classifier with high efficiency on the e^\pm signal. The remaining amount of proton background is evaluated using the information of the independent TRD subdetector. The reference shapes of the Probability Density Functions (P.D.F.) for the energy deposits in the TRD subdetector for the e^\pm and proton hypotheses are fit to the data using a standard template-fit procedure to measure the yield of $(e^+ + e^-)$ events, N , and the statistical uncertainty on N and on the number of background protons (Fig. 2). For all the analyses, the stability of the result has been checked by varying in a wide range of parameters the requirements used to select e^\pm and by modifying the shapes of the templates according to statistical fluctuations. The spread of

the results defines the systematic uncertainty on N , that is negligible at low energies and dominates the total systematic uncertainty above 500 GeV for the $(e^+ + e^-)$ flux measurement.

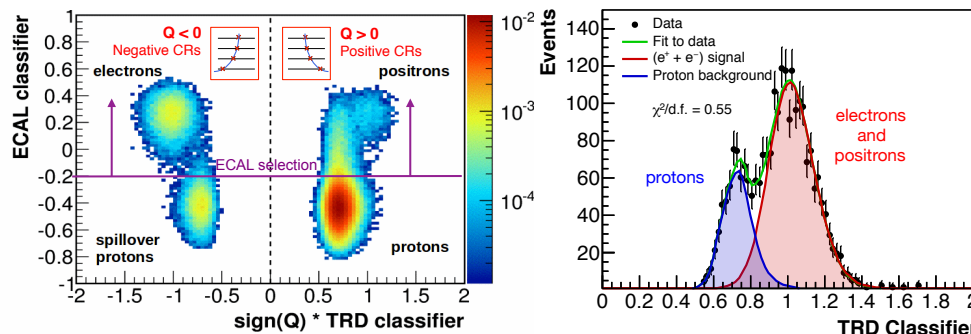


Figure 2: Left: TRD and ECAL classifier distributions for the 150 GeV $|Z|=1$ flight data sample. The violet line represents the selection on the ECAL shower shape to reject the majority of protons. Right: The tiny remaining proton background is estimated exploiting the independent TRD information. A template fit of the e^\pm and proton TRD classifier distributions to the data yields the amount of $(e^+ + e^-)$ in the sample.

The PF and the separate e^\pm flux measurements require additional quality selections on the reconstructed track to reduce the charge confusion (CC), the fraction of events with wrong measured curvature sign. CC is originated by the finite tracker resolution, multiple scattering and the production of secondary tracks by interaction of the primary particles with the detector material. The amount of CC has been estimated in data using E/R and a multi-variate estimator based on the information of the noise and the off-track energy deposits in the tracker planes. The CC amounts to $\sim 10\%$ at 500 GeV. For the PF measurement, the number of e^- and e^+ events has been evaluated using a 2D template-fit to the distributions of the TRD estimator and of E/R. For the separate e^\pm flux measurements, the number of e^- and e^+ events has been evaluated in a two-step procedure: the number of e^\pm extracted with a template-fit procedure to the TRD estimator in the positive and negative rigidity samples has been corrected by the amount of CC estimated with a template-fit procedure on the charge confusion estimator. The uncertainty on the CC is evaluated by a comparison between the CC evaluated in the flight data and in the Monte Carlo simulation of the physics processes and detector signals, and it dominates the systematic uncertainty for the PF measurement at high energies.

The acceptance for e^\pm passing through the AMS-02 active volumes has been evaluated using the Monte Carlo simulation. The geometric acceptance for e^\pm amounts to $\sim 550 \text{ cm}^2 \text{ sr}$. The differences observed between the efficiency of each requirement for the e^\pm selection in the flight data and in the simulation define the uncertainty on the e^\pm acceptance, that amounts to 2% above 3 GeV for the $(e^+ + e^-)$ flux measurement and dominates the systematic uncertainty up to $\sim 500 \text{ GeV}$.

The trigger efficiency, ϵ_{trig} , has been determined from data using a dedicated, unbiased trigger stream. It amounts to 100% above 3 GeV and decreases down to 75% at 1 GeV.

The calorimeter energy scale has been calibrated during a test beam at CERN with e^\pm beams from 10 GeV to 290 GeV. In space, the energy scale is monitored using the energy deposit of minimum ionizing particles and by the comparison between the ECAL energy and the tracker momentum measurements (E/R) for e^\pm . The ECAL energy scale is known with a precision of 2% in the test beam energy range, and it increases up to 5% at 0.5 GeV and at 1 TeV.

3. Results

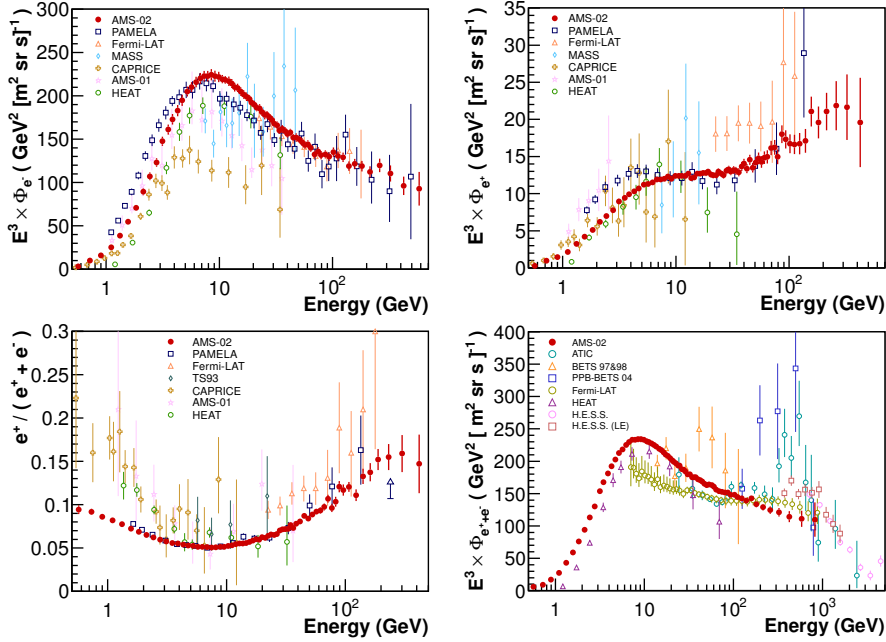


Figure 3: In red, AMS-02 measurements of the e^- flux (top-left), of the e^+ flux (top-right), of the positron fraction (bottom-left) and of the $(e^+ + e^-)$ flux (bottom-right). References in [1].

The fluxes of e^+ and e^- have been measured by AMS-02 up to, respectively, 500 GeV and 700 GeV. The e^\pm fluxes both harden with increasing energy above 20 GeV, but the e^- flux results softer than the e^+ flux. The PF, measured by AMS-02 up to 500 GeV, provides more sensitive information on the e^+ flux hardening. The PF rises up to ~ 200 GeV. Above this energy, the PF does no longer increase with energy. The PF maximum has been measured to be at 275 ± 32 GeV. These observations are not consistent with the expected production of e^+ from interactions of CRs with the interstellar gas, but they hint to the existence of an additional primary e^\pm source, like DM annihilation or production in nearby pulsars, or of unconventional acceleration and propagation mechanisms [3]. Additional distinct information is provided by the independent measurement of the $(e^+ + e^-)$ flux, with improved statistical and systematic uncertainties with respect to the separate e^\pm flux measurements. AMS-02 has measured the $(e^+ + e^-)$ flux up to 1 TeV. No features have been observed in the flux, and the $(e^+ + e^-)$ spectrum can be described by a single power law above 30 GeV, with spectral index $\gamma = -3.170 \pm 0.008(\text{stat+syst}) \pm 0.008(\text{en. scale})$ determined with accuracy better than 1%.

These results are based on 10.6 million e^\pm events collected in the first 30 months of operations, and corresponding to $\sim 15\%$ of the expected data sample for the whole AMS mission. Complementary measurements of different CR channels are essential to identify the dominant source of the e^\pm excess. The recent measurement of the \bar{p} flux up to 450 GeV by AMS-02 provides complementary and sensitive information for the search of signatures of DM annihilation in the Galaxy [4]. AMS-02 is also measuring the fluxes of protons and light nuclei [5] whose features are useful to

understand the properties of the galactic propagation environment and to consequently improve the knowledge of the astrophysical backgrounds for the search of new CR sources.

AMS-02 is now collecting data for more than 5 years. The new data will increase the accuracy of the e^\pm measurements, improving the sensitivity to the searches of additional sources of CRs, and will increase the maximum energy reach of the measurements. AMS-02 will collect data at least until 2024, measuring the fluxes of e^- and e^+ up to 1 TeV.

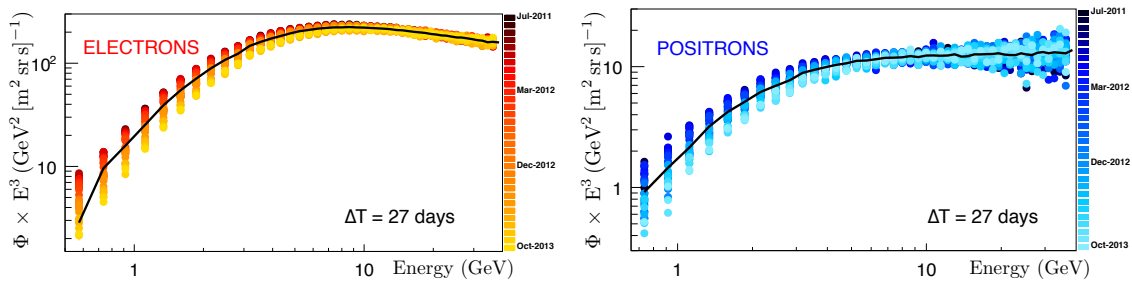


Figure 4: Time dependence of the low energy e^\pm fluxes measured by AMS-02.

AMS-02 is also measuring the time dependence of different CR species at low energies. Fig. 4 shows the measurement of the low energy e^\pm fluxes as function of the measuring time. The amount of statistics and the particle identification properties allow AMS-02 to monitor the time dependence of low energy CRs with unprecedented accuracy, providing important information for the understanding of the local Solar environment and the propagation of low energy CRs in the heliosphere, with additional information on the dependence of such phenomena on the sign of the charge of CRs. At the end of its mission, AMS-02 will be able to provide for the first time the detailed time dependence of e^+ and e^- fluxes during an entire 11-year solar cycle.

Acknowledgments

This work has been supported by acknowledged persons and institutions in AMS-02 publication[1, 2, 4, 5], as well as by the Italian Space Agency under ASI-INFN Agreement No. 2013-002-R.0.

References

- [1] L. Accardo *et al*, *Phys. Rev. Lett.* **113**, 121101 (2014); M. Aguilar *et al*, *Phys. Rev. Lett.* **113**, 121102 (2014); M. Aguilar *et al*, *Phys. Rev. Lett.* **113**, 221102 (2014).
- [2] M. Aguilar *et al*, *Phys. Rev. Lett.* **110**, 141102 (2013).
- [3] L. Feng *et al.*, *Phys. Lett.* **B 728** (2014) 250; K. Blum *et al.*, *Phys. Rev. Lett.* **111** (2013) 211101; L. Bergström *et al.*, *Phys. Rev. Lett.* **111** (2013) 171101; I. Cholis and D. Hooper, *Phys. Rev.* **D 88** (2013) 023013; T. Linden and S. Profumo, *Astrophys. J.* **772** (2013) 18.
- [4] M. Aguilar *et al*, *Phys. Rev. Lett.* **117**, 091103 (2016); A. Chen, in proceedings of ICHEP 2016, [PoS \(ICHEP2016\) 071](#) (2016)
- [5] M. Aguilar *et al*; *Phys. Rev. Lett.* **114**, 171103 (2015). M. Aguilar *et al* *Phys. Rev. Lett.* **115**, 211101 (2015); A. Oliva, in proceedings of ICHEP 2016, [PoS \(ICHEP2016\) 072](#) (2016)